J. Fluid Mech. (1990), *vol.* 210, *pp.* 459–473
Printed in Great Britain

Streaming from a sphere due to a pulsating source

By NORSARAHAIDA AMIN AND N. RILEY
School of Mathematics, University of East Anglia, Norwich, UK

(Received 31 January 1989)

The steady streaming outside the Stokes shear-wave layer, which forms on the surface of a sphere when placed close to an oscillatory point source, is considered. Particular attention is devoted to the case of high streaming Reynolds-number flow. Thin circular jets, analogous to the plane jets known to occur in two-dimensional flow, are predicted and visualized by means of a simple experiment.

1. Introduction

The phenomenon of acoustic streaming may arise in any fluctuating flow. Studies of it date back to the pioneering work of Rayleigh (1884), work that has been continued *inter alia* by Schlichting (1955), Nyborg (1953) and Westervelt (1953). Lighthill (1978) has clearly demonstrated the fundamental principle that it is the attenuation of acoustic energy flux that makes momentum flux available to force the streaming motion. Such attenuation may take place in the main body of the fluid, as for example in an ultrasonic beam, or in the neighbourhood of a solid boundary owing to fluid friction. The example considered herein is of the latter type. We consider the flow over a sphere of radius a, due to an oscillatory point source placed at a distance aR from its centre ($R > 1$).

The flow is characterized by a streaming Reynolds number R_s, based upon the time-independent component of the fluid velocity. Stuart (1963), in the context of the flow induced by a vibrating cylinder, first recognized the importance of this parameter, particularly for flows in which $R_s \gg 1$. Subsequently Riley (1967) demonstrated that when $R_s = O(1)$ the steady streaming outside the Stokes shear-wave layer which forms at the surface of the vibrating cylinder is governed by the Navier–Stokes equations for steady flow. This result owes its origin to the fact that the Reynolds stresses which drive the steady streaming only act directly within the Stokes layer, and influence the flow outside it indirectly through the persistence of a streaming component at its edge. For $R_s \gg 1$ Stuart (1966) predicted that a jet-like streaming flow, along the axis of oscillation, would originate at the cylinder. Davidson & Riley (1972) have demonstrated the existence of such a jet in flow-visualization pictures from which it was possible to make quantitative measurements of the jet flow.

In a recent paper Riley (1987) has considered the steady streaming when an oscillatory line source is placed close, and parallel, to the generators of a circular cylinder. With $R_s \gg 1$, jet-like flows along the axis of symmetry are again predicted, with a much weaker jet on the leeward side of the cylinder. This problem first attracted the attention of Wang (1972) who was concerned only with the case $R_s \ll 1$ although, as Lighthill (1978) has emphasized, all really noticeable acoustic streaming motions are associated with $R_s \gg 1$. Wang (1982) also considered the situation which forms the basis for the present paper, namely the steady streaming

from a sphere close to an unsteady source, where he was again concerned only with the case $R_s \ll 1$. In our work we first set out, in §2, the solution for the basic unsteady flow both within, and outside, the Stokes layer which forms at the surface of the sphere. In §3 we address the problem of the induced steady streaming. First, with $R_s \ll 1$, we correct a numerical error in Wang's work on the basis of which he incorrectly predicts an increasing multiplicity of steadily recirculating cells as the source approaches the sphere. But our main concern is with the case $R_s \gg 1$. We trace the streaming boundary-layer flow over the sphere, which develops outside the Stokes layer, up to the two stagnation points that form along the line joining the source location to the sphere centre. We pay particular attention to the singularity in the boundary-layer solution at these two points as the flow erupts along the axis of symmetry. The flow along this axis of symmetry, weaker on the leeward than the windward side in relation to the source position, is in the nature of a thin circular jet. In an appropriate limit where the source goes to infinity, as does its strength, the flow over the sphere is equivalent to that induced by a vibrating sphere in a fluid which is otherwise at rest. Since the appearance of the thin circular jets, described above, does not seem to have been previously recorded (although their two-dimensional analogues are well documented, for example by Davidson & Riley 1972; Haddon & Riley 1979), we have carried out a simple experiment to demonstrate their presence. This is described briefly in §4, and is limited to a visualization of the jets in question.

2. The primary unsteady solution

We consider the flow induced over a sphere of radius a when a point source of strength $m\cos\omega t'$ is placed at a distance aR ($R > 1$) from the centre of the sphere, in a fluid which is otherwise at rest. In a spherical polar coordinate system with origin at the centre of the sphere the source is at $(aR, 0, 0)$. With the scales of velocity, stream function, radial distance and time chosen as m/a^2R^2, m/R^2, a and ω^{-1} respectively the equation satisfied by the stream function ψ is

$$\frac{\partial}{\partial t}(\mathrm{D}^2\psi)+\frac{\epsilon}{r^2}\left\{\frac{\partial(\psi,\mathrm{D}^2\psi)}{\partial(r,\mu)}+\frac{2}{r^2}\mathrm{D}^2\psi\mathrm{L}\psi\right\}=\frac{\epsilon^2}{R_s}\mathrm{D}^4\psi, \tag{1}$$

where $$\mu=\cos\theta, \quad \mathrm{D}^2=\frac{\partial^2}{\partial r^2}+\frac{1-\mu^2}{r^2}\frac{\partial^2}{\partial\mu^2}, \quad \mathrm{L}=\frac{\mu}{1-\mu^2}\frac{\partial}{\partial r}+\frac{1}{r}\frac{\partial}{\partial\mu},$$

and the velocity components are given by

$$v_r=\frac{1}{r^2\sin\theta}\frac{\partial\psi}{\partial\theta}, \quad v_\theta=-\frac{1}{r\sin\theta}\frac{\partial\psi}{\partial r}. \tag{2}$$

In (1) the parameters ϵ, R_s are defined as

$$\epsilon=\frac{m}{\omega a^3R^2}, \quad R_s=\frac{m^2}{a^4R^4\omega\nu}. \tag{3}$$

We assume the parameter ϵ, which provides a measure of the ratio of fluid particle displacements to the radius of the sphere, to be small throughout, and R_s, the appropriate Reynolds number of the induced steady streaming with velocity

$O(\epsilon m/a^2R^2)$, to be an order one quantity. Formally, we are concerned with the development of a solution in which

$$\lim_{\epsilon\to 0} R_s = O(1).$$

The boundary conditions at the sphere require v_r, v_θ to vanish there, and the stream function must exhibit appropriate source-like behaviour at $(R, 0, 0)$.

With terms $O(\epsilon)$ in (1) ignored, the leading-order solution ψ_0 satisfies $\partial(\mathrm{D}^2\psi_0)/\partial t = 0$, and the periodic solution of this equation which satisfies $v_r = 0$, at $r = 1$, is

$$\psi_0 = R^2\left\{\frac{R-r\mu}{(r^2-2Rr\mu+R^2)^{\frac{1}{2}}} - 1 + r + \frac{r\mu - Rr^2}{(R^2r^2-2Rr\mu+1)^{\frac{1}{2}}}\right\} e^{it}, \tag{4}$$

where here, and below, the real part of any complex quantity is to be understood.

The stream function (4) consists of the source at $(R, 0, 0)$ together with its image in the sphere which comprises a source at the inverse point, and a uniform line sink between that point and the centre of the sphere. We note that as $R \to \infty$,

$$\psi_0 \sim \tfrac{1}{2}(1/r - r^2)(1-\mu^2)\, e^{it}. \tag{5}$$

This is the stream function which is appropriate to a sphere vibrating in a fluid that is otherwise at rest. Some aspects of this flow have been considered by Riley (1966).

The solution (4), which is inviscid and irrotational, does not satisfy the no-slip condition at $r = 1$. The adjustment of the slip velocity takes place in a thin Stokes shear-wave layer. We introduce this by writing

$$\Psi = \frac{R_s^{\frac{1}{2}}}{\sqrt{2\epsilon}}\psi, \quad \eta = \frac{R_s^{\frac{1}{2}}}{\sqrt{2\epsilon}}(r-1), \tag{6}$$

and in this layer the leading-order term satisfies

$$\frac{\partial}{\partial t}\left(\frac{\partial^2 \Psi_0}{\partial \eta^2}\right) = \frac{1}{2}\frac{\partial^4 \Psi_0}{\partial \eta^4}. \tag{7}$$

The solution of (7) which satisfies the no-slip condition, and matches with (4), is

$$\Psi_0 = R^2 C(\mu) f(\eta)\, e^{it}, \tag{8}$$

where $$C(\mu) = 1 - \frac{(R^3 - 3R^2\mu + 3R - \mu)}{(R^2-2R\mu+1)^{\frac{3}{2}}}, \quad f(\eta) = \eta - \tfrac{1}{2}(1-i)\{1 - e^{-(1+i)\eta}\}.$$

The outer and inner solutions (4), (8) represent the primary fluctuating flow. The Reynolds stresses associated with this flow, in the Stokes layer, are responsible for the induced steady streaming which we now consider.

3. The induced steady streaming

It has been well-established, see for example Riley (1967), that for flows of the type under consideration here the steady streaming originates within the Stokes layer owing to the action of Reynolds stresses. We write

$$\Psi = \Psi_0 + \epsilon(\Psi_1^{(u)} + \Psi_1^{(s)}) + O(\epsilon^2), \tag{9}$$

and we note that in (9) we have already anticipated that at $O(\epsilon)$ the flow will consist of a fluctuating part (superscript u), and a time-independent part (superscript s). Our

main concern is the steady part of (9). If we substitute (6), (9) into equation (1) then at $O(\epsilon)$ we have, as the equation for $\Psi_1^{(s)}$,

$$\frac{\partial^4 \Psi_1^{(s)}}{\partial \eta^4} = \left\{ 2\frac{\partial(\Psi_0, \partial^2 \Psi_0/\partial\eta^2)}{\partial(\eta,\mu)} + \frac{4\mu}{1-\mu^2}\frac{\partial^2 \Psi_0}{\partial \eta^2}\frac{\partial \Psi_0}{\partial \eta} \right\}^{(s)}$$

$$= 2R^4 C(\mu)\left\{ C'(\mu)(\dot{f}\ddot{f}+f\dddot{f}) + \frac{2\mu}{1-\mu^2}C(\mu)\ddot{f}\dddot{f} \right\}. \tag{10}$$

In (10) a prime denotes differentiation with respect to μ, a dot with respect to η. The required solution of (10) is

$$\Psi_1^{(s)} = \tfrac{1}{2}R^4 C(\mu)\Big[C'(\mu)\{-i\eta\, e^{-(1+i)\eta} - (2i+3)\, e^{-(1+i)\eta} - \tfrac{1}{4}e^{-2\eta} + \tfrac{13}{4} - \tfrac{3}{2}\eta\}$$

$$+ \frac{\mu}{1-\mu^2}C(\mu)\{-(1+i)\, e^{-(1+i)\eta} - \tfrac{1}{4}e^{-2\eta} + \tfrac{5}{4} - \tfrac{1}{2}\eta\}\Big], \tag{11}$$

which has previously been presented by Wang (1982). We note from (11) that

$$\frac{\partial \Psi_1^{(s)}}{\partial \eta} \sim -\tfrac{1}{4}R^4 C(\mu)\left\{ 3C'(\mu) + \frac{\mu}{1-\mu^2}C(\mu) \right\} \quad \text{as } \eta \to \infty, \tag{12}$$

so that the steady streaming persists at $O(\epsilon)$ beyond the Stokes layer.

In the outer region we write, corresponding to (9),

$$\psi = \psi_0 + \epsilon(\psi_1^{(u)} + \psi_1^{(s)}) + \epsilon^2\psi_2 + \epsilon^3\psi_3 + O(\epsilon^4). \tag{13}$$

Again, it is the steady streaming represented by $\psi_1^{(s)}$ in (13) that is of greatest interest to us. Upon substitution of (13) into (1) it has been shown by Riley (1966, 1967) that an equation for $\psi_1^{(s)}$ emerges only when terms $O(\epsilon^3)$ are considered. The appropriate equation has been derived by Riley (1966) as

$$\frac{R_s}{r^2}\left\{ \frac{\partial \psi_1^{(s)}}{\partial r}\frac{\partial}{\partial \mu}(\mathrm{D}^2\psi_1^{(s)}) - \frac{\partial \psi_1^{(s)}}{\partial \mu}\frac{\partial}{\partial r}(\mathrm{D}^2\psi_1^{(s)}) + 2\mathrm{L}\psi_1^{(s)}\,\mathrm{D}^2\psi_1^{(s)} \right\} = \mathrm{D}^4\psi_1^{(s)}. \tag{14}$$

Equation (14) shows that $\psi_1^{(s)}$ is to be determined from the complete Navier–Stokes equations with Reynolds number R_s, which as we have noted earlier and now clearly see, is the Reynolds number that characterizes the steady streaming. The boundary conditions which $\psi_1^{(s)}$ must satisfy are

$$\psi_1^{(s)} = 0, \quad \frac{\partial \psi_1^{(s)}}{\partial r} = -\tfrac{1}{4}R^4 C(\mu)\left\{ 3C'(\mu) + \frac{\mu}{1-\mu^2}C(\mu) \right\} = F(\mu), \quad \text{say, on } r = 1, \tag{15a, b}$$

as required by matching with the Stokes layer, and

$$\psi_1^{(s)} \sim o(r^2) \quad \text{as } r \to \infty. \tag{16}$$

We consider next the solution of (14), subject to (15), (16) in the limiting cases of small and large streaming Reynolds numbers R_s respectively.

(i) $R_s \ll 1$

The governing equation, from (14), is $\mathrm{D}^4\psi_1^{(s)} = 0$, and the solution of this equation which satisfies (15a) and (16) is

$$\psi_1^{(s)} = \sum_{n=1}^{\infty} B_n(r^{-n} - r^{-n+2})\, Q_n(\mu), \tag{17}$$

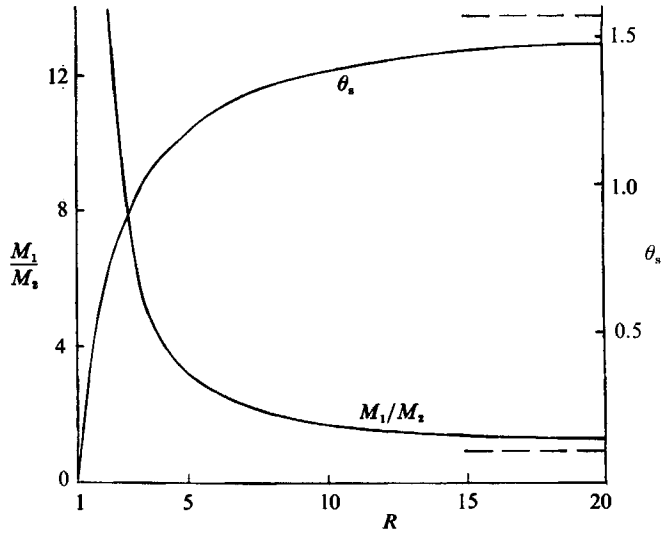

FIGURE 1. In this figure we show the stagnation point of attachment θ_s, which is determined from $F(\mu) = 0$, where $F(\mu)$ is defined in (15*b*), and is independent of R_s. Also shown is the momentum flux ratio M_1/M_2 for $R_s \gg 1$, where M is defined in (24). In each case the broken line represents the limit as $R \to \infty$.

where
$$Q_n(\mu) = \int_{-1}^{\mu} P_n(x)\,\mathrm{d}x, \tag{18}$$

and $P_n(\mu)$ is the Legendre polynomial of degree n. The solution is completed by the determination of the constants B_n from the condition (15*b*). From (17), (18) this gives

$$\sum_{n=1}^{\infty} B_n P_n(\mu) = -\tfrac{1}{2}F'(\mu),$$

so that
$$B_n = -\frac{2n+1}{4}\int_{-1}^{1} F'(\mu)\,P_n(\mu)\,\mathrm{d}\mu$$
$$= \frac{2n+1}{4}\int_{-1}^{1} F(\mu)\,P_n'(\mu)\,\mathrm{d}\mu, \tag{19}$$

since $F(\pm 1) = 0$. For all the examples we have considered it has not been necessary to use more than 40 terms of the series (17).

The solution (17) has been previously given by Riley (1966) for the special case $R = \infty$, which corresponds to (5), and by Wang (1982) for finite values of R. The latter author expresses the solution in terms of Gegenbauer polynomials; however we have preferred to work with the more familiar Legendre polynomials. Wang has suggested that as R decreases towards unity the character of the steady streaming changes, and becomes multi-cellular in form. He illustrates this by a streaming pattern for $R = 3$, and remarks that the multi-cellularity increases when the source is moved even closer to the sphere. This proposition is, however, incorrect. In addition to vanishing at $\mu = \pm 1$, $F(\mu)$ has only one zero in the interval $-1 < \mu < 1$, at $\mu = \mu_s$ say, for all values of R. The outer flow has, therefore, only one stagnation point on $r = 1$, at $\theta = \theta_s$, in addition to the stagnation points at $\theta = 0, \pi$. Wang's error may be traced to an error in his evaluation of B_4 for $R = 3$, the published value of which overestimates the correct value by a factor of 10.

In figure 1 we show the variation of θ_s with R. As $R \to 1$ the stagnation point $\theta = \theta_s$ moves closer to $\theta = 0$ and, as may be expected, the steady streaming becomes increasingly vigorous in the region $0 \leqslant \theta \leqslant \theta_s$. Streamline patterns associated with the outer steady streaming $\psi_1^{(s)}$ are shown in figure 2 for various values of R.

(ii) $R_s \gg 1$

In this case the flow outside the Stokes shear-wave layer does itself exhibit boundary-layer behaviour. The outer boundary layer is of thickness $O(R_s^{-\frac{1}{2}})$, and in it we write

$$\psi_1^{(s)} = R_s^{-\frac{1}{2}} \tilde{\psi}_1^{(s)}, \quad r - 1 = R_s^{-\frac{1}{2}} y. \tag{20}$$

When the variables (20) are introduced into (14) we recover the appropriate boundary-layer equation for $\tilde{\psi}_1^{(s)}$. However we find it convenient to integrate this once with respect to y, and introduce the velocity components $u = v_\theta^{(s)}$, $v = R_s^{\frac{1}{2}} v_r^{(s)}$ where $v_r^{(s)}$, $v_\theta^{(s)}$ are related to $\psi_1^{(s)}$ as in (2). The equations satisfied by u, v are, then,

$$\left.\begin{aligned} \frac{\partial}{\partial \theta}(u \sin\theta) + \frac{\partial}{\partial y}(v \sin\theta) = 0, \\ u\frac{\partial u}{\partial \theta} + v\frac{\partial u}{\partial y} = \frac{\partial^2 u}{\partial y^2}, \end{aligned}\right\} \tag{21a, b}$$

which are the conventional boundary-layer equations. The boundary conditions to be satisfied are

$$u \to 0 \quad \text{as } y \to \infty, \tag{22}$$

together with a condition of matching with the Stokes layer

$$v = 0, \quad u = u_e = -F(\cos\theta)/\sin\theta, \tag{23}$$

where F is defined in (15b). In figure 3 we show u_e as a function of θ for various values of R. The numerical solution of (21) commences at the stagnation point $\theta = \theta_s$, and is carried out using the numerical method adopted, and fully described, by Potter & Riley (1980) and Awang (1984) for the free-convective boundary-layer flow over a sphere. For $\theta > \theta_s$ where $u_e > 0$ we introduce the variable $\bar{\theta} = \theta - \theta_s$ into (21); the integration then proceeds from $\bar{\theta} = 0$ in the direction of $\bar{\theta}$ increasing. For $\theta < \theta_s$, where $u_e < 0$, we define new variables $\tilde{\theta} = \theta_s - \theta$, $\tilde{u} = -u$ in (21); the integration then proceeds from $\tilde{\theta} = 0$ to $\tilde{\theta} = \theta_s$.

A feature of the solution is that the momentum flux in the boundary layer is non-zero as $\theta \to 0, \pi$. The momentum flux is given by

$$M(\theta) = 2\pi \int_0^\infty u^2 \sin\theta \, dy. \tag{24}$$

We define $M_1 = M(0), M_2 = M(\pi)$, and in figure 1 we show the variation of M_1/M_2 with R. We note that the momentum flux ratio increases dramatically as the source approaches the sphere. This is as in the case of two-dimensional flow, but there is a marked difference in the nature of the two flows as the streaming boundary layers approach their terminal points. In the planar case the results obtained by Riley (1987), for the flow over a circular cylinder, show no unusual behaviour in the boundary layer as the equatorial plane is reached, at which point the boundary layers collide to emerge as a plane, free jet. The present situation is different as we may infer at once from (24). For M to remain finite as $\theta \to 0, \pi$ the boundary-layer solution must clearly exhibit some singular behaviour. This singular behaviour is not dissimilar to that discussed by Potter & Riley (1980), and Brown & Simpson (1982)

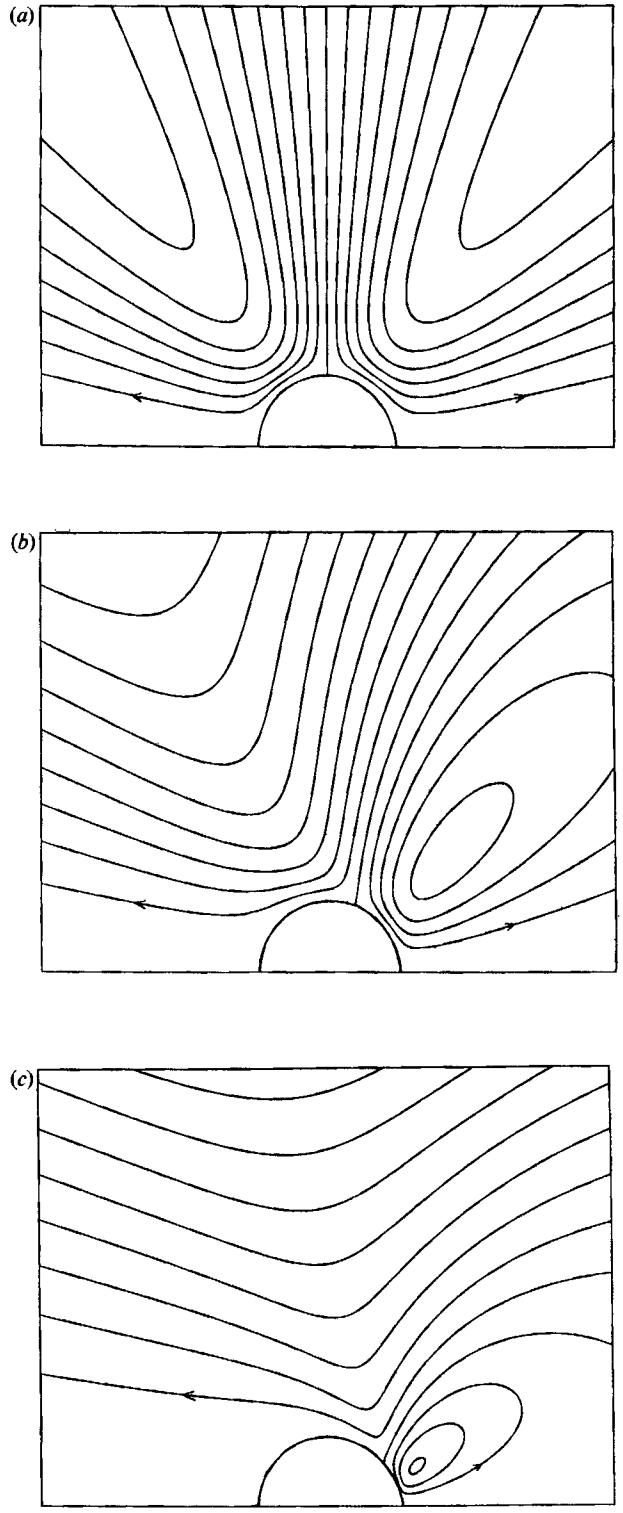

FIGURE 2. The outer flow mean streamlines for $R_s \ll 1$. In each case the streamlines are plotted at equal intervals $\delta\psi$ of $\psi_1^{(s)}$. (*a*) $R = \infty, \delta\psi = 0.05$; (*b*) $R = 5, \delta\psi = 0.1$; (*c*) $R = 2, \delta\psi = 0.25$.

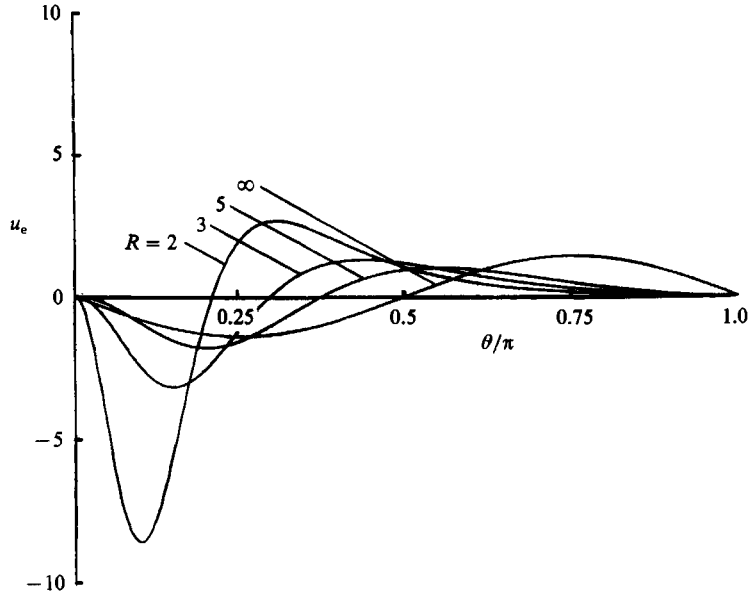

FIGURE 3. The slip velocity u_e, defined in equation (23), for various values of R.

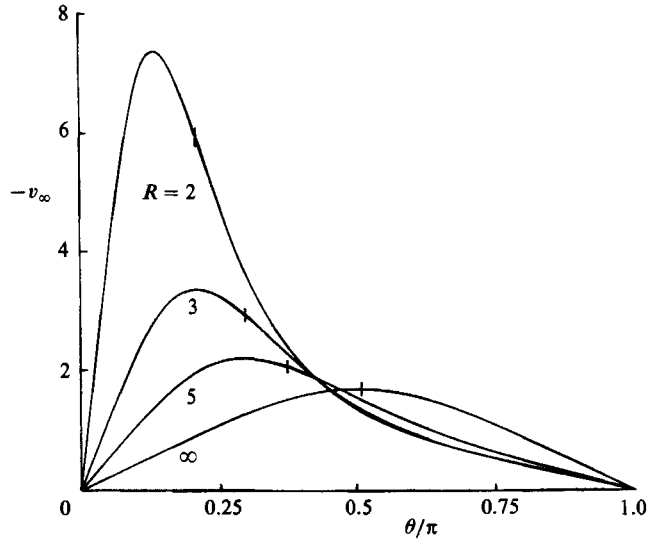

FIGURE 4. The entrainment velocity v_∞, in the case $R_s \gg 1$, for various values of R. The stagnation point θ_s is denoted in each case by a bar on the curve.

for free-convective flow over a sphere, and is associated with the convergence of the boundary layer to the points $\theta = 0, \pi$ in the three-dimensional case. We now consider the behaviour of the solution close to these points.

First, from equation (21*b*) we see that if $v \to v_\infty(\theta)$ as $y \to \infty$ then we have, in that limit,

$$v_\infty \frac{\partial u}{\partial y} = \frac{\partial^2 u}{\partial y^2},$$

with solution $\partial u/\partial y = A(\theta)\, e^{v_\infty y}$. To satisfy (22) we require $v_\infty(\theta) < 0$. This result is confirmed in figure 4 where we show v_∞ as a function of θ for various values of R.

Again we note the increasing vigour of the flow, on the 'source-side' of the sphere, as the source approaches the sphere. Initially the velocity component v is everywhere negative within the boundary layer. The first sign of any difficulty is when a change of sign of v takes place within the boundary layer. As the terminal points $\theta = 0, \pi$ are approached, this region of positive normal velocity spreads across the boundary layer, and becomes unbounded in the limits $\theta \to 0, \pi$. This is the precursor to the eruption of the boundary layers which takes place at the terminal points, and we now examine it in more detail in the vicinity of $\theta = 0$.

Guided by our numerical calculations in which u remains finite, but the boundary-layer thickness increases indefinitely, we write

$$u = \bar{u}(\bar{\eta}), \quad v = \bar{v}(\bar{\eta})\,\Delta(\theta), \quad \bar{\eta} = \{y + \bar{\mu}(\theta)\}/\delta(\theta), \tag{25}$$

where $|\delta|^{-1}, |\Delta|^{-1}, |\bar{\mu}| \ll 1$ for small θ. Substitution of (25) into (21) gives, at leading order,

$$\bar{u} - \theta\frac{\dot{\delta}}{\delta}\bar{\eta}\bar{u}' + \frac{\theta\Delta}{\delta}\bar{v}' = 0, \quad \bar{v} = \bar{\eta}\bar{u}\frac{\dot{\delta}}{\Delta}, \tag{26}$$

where now a prime and a dot denote differentiation with respect to $\bar{\eta}$, θ respectively, and we have made the additional assumption that $\theta^2|\dot{\bar{\mu}}| \ll 1$. For non-zero $\bar{u}$, elimination of $\bar{v}$ from (26) shows that $\theta\dot{\delta} + \delta = 0$, from which we have $\delta = \theta^{-1}$ and $\Delta = \theta^{-2}$ so that

$$u = G\{(y+\bar{\mu})\,\theta\}, \quad v = -(y+\bar{\mu})\,G\{(y+\bar{\mu})\,\theta\}/\theta. \tag{27}$$

The function $G(\bar{\eta})\,(< 0)$ depends upon conditions upstream, and can only be determined completely from the step-by-step integration of (21).

The solution (27) is inviscid in character, and we now analyse the flow in a region close to the boundary where viscous effects are important. Our analysis follows that of Brown & Simpson (1982). We note that as $\theta \to 0, u_e \sim -k\theta$, where k is a constant, and we write $u = -k\theta + u^*$ such that $u^* = 0$ on $y = 0$. In equations (21) we now introduce new independent variables $\{\tilde{\mu}(\theta), \tilde{\eta}\}$ where $\tilde{\eta} = y\tilde{\mu}^{\frac{1}{3}}$, and we write $u^* = -\theta\tilde{\mu}^{\frac{2}{3}}U, v = \tilde{\mu}^{\frac{1}{3}}V$; $\tilde{\mu}(\theta)$ is not determined at this stage but is assumed to be large. From (21) the equations satisfied by U, V are

$$\left.\begin{aligned} &2U - \frac{\partial V}{\partial\tilde{\eta}} + 2k\tilde{\mu}^{-\frac{2}{3}} - \tfrac{2}{3}\tilde{\delta}U - \tfrac{1}{3}\tilde{\delta}\tilde{\eta}\frac{\partial U}{\partial\tilde{\eta}} - \tilde{\delta}\tilde{\mu}\frac{\partial U}{\partial\tilde{\mu}} = 0, \\ &\frac{\partial^2 U}{\partial\tilde{\eta}^2} - V\frac{\partial U}{\partial\tilde{\eta}} + U^2 + 2k\tilde{\mu}^{-\frac{2}{3}}U - \tilde{\delta}\left(\tfrac{2}{3}U^2 + \tfrac{1}{3}\tilde{\eta}U\frac{\partial U}{\partial\tilde{\eta}} + \tilde{\mu}U\frac{\partial U}{\partial\tilde{\mu}}\right) \\ &\qquad - k\tilde{\delta}\tilde{\mu}^{-\frac{2}{3}}\left(\tfrac{2}{3}U + \tfrac{1}{3}\tilde{\eta}\frac{\partial U}{\partial\tilde{\eta}} + \tilde{\mu}\frac{\partial U}{\partial\tilde{\mu}}\right) + k^2\tilde{\mu}^{-\frac{4}{3}} = 0. \end{aligned}\right\} \tag{28}$$

In equations (28) $\tilde{\mu}\tilde{\delta} = -\theta\,\mathrm{d}\tilde{\mu}/\mathrm{d}\theta$ and we assume $\tilde{\delta} \ll 1$, an assumption which may be verified *a posteriori*. We now write

$$\left.\begin{aligned} U &= \tilde{\eta} + \tilde{\mu}^{-\frac{2}{3}}U_1(\tilde{\eta}) + \tilde{\mu}^{-\frac{4}{3}}U_2(\tilde{\eta}) + \ldots, \\ V &= \tilde{\eta}^2 + \tilde{\mu}^{-\frac{2}{3}}V_1(\tilde{\eta}) + \tilde{\mu}^{-\frac{4}{3}}V_2(\tilde{\eta}) + \ldots. \end{aligned}\right\} \tag{29}$$

Upon substitution of (29) into (28) we see that $U_1(\tilde{\eta}), V_1(\tilde{\eta})$ satisfy

$$\left.\begin{aligned} V_1' &= 2U_1 + 2k - \tilde{\delta}\tilde{\mu}^{\frac{2}{3}}\tilde{\eta}, \\ U_1'' - \tilde{\eta}^2U_1' + 2\tilde{\eta}U_1 + 2k\tilde{\eta} - \tilde{\delta}\tilde{\mu}^{\frac{2}{3}}\tilde{\eta}^2 &= V_1, \end{aligned}\right\} \tag{30a, b}$$

where a prime denotes differentiation with respect to $\tilde{\eta}$. If we eliminate V_1 between (30a, b) the resulting equation for U_1 may be integrated once to give

$$U_1'' = -\tilde{\delta}\tilde{\mu}^{\frac{2}{3}} e^{\frac{1}{3}\tilde{\eta}^3} \int_{\tilde{\eta}}^{\infty} t e^{-\frac{1}{3}t^3} dt. \tag{31}$$

But since $U_1''(0)$ is required to vanish we infer from (31) that $\tilde{\delta}\tilde{\mu}^{\frac{2}{3}} \ll 1$ and so $U_1 = a_1\tilde{\eta}, V_1 = a_1\tilde{\eta}^2 + 2k\tilde{\eta}$, where a_1 is a constant. At next order we have, as equations for $U_2(\tilde{\eta}), V_2(\tilde{\eta})$

$$\left.\begin{aligned} V_2' &= 2U_2 - \tilde{\delta}\tilde{\mu}^{\frac{4}{3}}\tilde{\eta}, \\ U_2'' - \tilde{\eta}^2 U_2' + 2\tilde{\eta}U_2 - \tilde{\delta}\tilde{\mu}^{\frac{4}{3}}\tilde{\eta}^2 + k^2 &= V_2, \end{aligned}\right\} \tag{32a, b}$$

from which we deduce, following the elimination of V_2, that

$$U_2'' = -\tilde{\delta}\tilde{\mu}^{\frac{4}{3}} e^{\frac{1}{3}\tilde{\eta}^3} \int_{\tilde{\eta}}^{\infty} t e^{-\frac{1}{3}t^3} dt. \tag{33}$$

Now, from (32b) we have $U_2''(0) = -k^2$ which gives, from (33), $\tilde{\delta}\tilde{\mu}^{\frac{4}{3}} = k^2 3^{\frac{1}{3}}/(-\frac{1}{3})! = \lambda_1$ say. We now have two relationships connecting $\tilde{\delta}(\theta), \tilde{\mu}(\theta)$ from which we may deduce that

$$\tilde{\mu}^{\frac{4}{3}} = \tfrac{4}{3}\lambda_1 \log(\lambda_2/\theta), \tag{34}$$

where λ_2 is arbitrary. The basic structure of the inner region which has just been established, is consistent with our numerical calculations and this may be demonstrated as follows. Define

$$\tau = \frac{1}{\theta}\frac{\partial u}{\partial y}\bigg|_{y=0} = \tilde{\mu}\frac{\partial U}{\partial \tilde{\eta}}\bigg|_{\tilde{\eta}=0} = \tilde{\mu} + O(\tilde{\mu}^{-\frac{2}{3}}),$$

so that $3\tau^{\frac{4}{3}} = 4\lambda_1 \log(\lambda_2/\theta)$, from (34), or

$$\frac{\theta}{\lambda_2} = \exp\left(-\frac{3\tau^{\frac{4}{3}}}{4\lambda_1}\right). \tag{35}$$

In figure 5 we show, for the case $R = \infty, k = \frac{45}{16}, \lambda_1 = 8.424$, the variation of $\exp(-3\tau^{\frac{4}{3}}/4\lambda_1)$ with θ, and confirm the linear prediction (35).

It remains to match this solution with our outer inviscid solution (27). This is straightforward although the manipulative details, set out in Amin (1989), are tedious and yield $\bar{\mu}(\theta) = k/\tilde{\mu}(\theta)$. The constant a_1 of U_1, is only determined following a more detailed investigation of the outer solution.

With the nature of the breakdown of the boundary-layer solution as $\theta \to 0$ established, we now examine the consequences of it for the eruption region in the neighbourhood of $r = 1, \theta = 0$ from which a jet emerges along the axis $\theta = 0$. We have noted that

$$v \sim -\bar{\eta}G(\bar{\eta})/\theta^2 \quad \text{as } \theta \to 0. \tag{36}$$

We interpret the rapid increase of v in the boundary layer as part of the flow realignment process since, as $\theta \to 0$, the radial component of velocity becomes parallel to the axis $\theta = 0$. On the velocity scale we have introduced, velocities in excess of $O(1)$ are not anticipated. We observe, from (36), that at a fixed $\bar{\eta}, v_r^{(s)} = R_s^{-\frac{1}{2}}v = O(1)$ when $\theta = O(R_s^{-\frac{1}{4}})$ at which point the thickness of the boundary layer on the scale of the sphere radius is $R_s^{-\frac{1}{2}}\delta = O(R_s^{-\frac{1}{4}})$. We have then an eruption region centred on $r = 1, \theta = 0$ of dimensions $R_s^{-\frac{1}{4}} \times R_s^{-\frac{1}{4}}$ on the scale of the sphere radius within which velocities are $O(1)$. Introducing these scales into the governing equation (14) for the steady streaming, we infer that the eruption region is essentially one of inviscid flow in which the vorticity is constant along the streamlines of the flow.

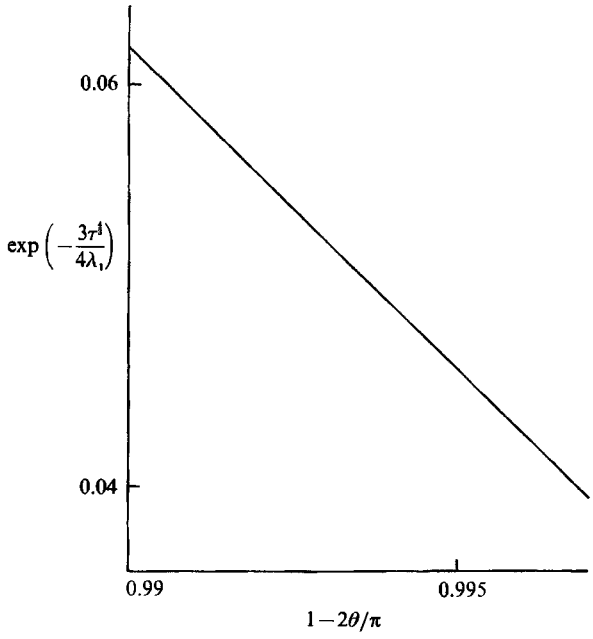

FIGURE 5. The function $\exp(-3\tau^{\frac{1}{3}}/4\lambda_1)$ calculated from the numerical results for $R_s \gg 1$, with $R = \infty$.

From the eruption region a thin round jet emerges along the axis $\theta = 0$. It is convenient, for the discussion of this, to introduce a cylindrical polar coordinate system (ρ, ϕ, z) in which the z-axis coincides with the axis $\theta = 0$ of our spherical polar coordinate system. The corresponding velocity components are $(v_\rho^{(s)}, 0, v_z^{(s)})$. As we have already determined, the steady streaming is governed by the Navier–Stokes equations at Reynolds number R_s. For large R_s we make the boundary-layer approximation in the jet so that $v_\rho^{(s)}, v_z^{(s)}$ satisfy

$$\left.\begin{aligned} \frac{\partial}{\partial z}(\rho v_z^{(s)}) + \frac{\partial}{\partial \rho}(\rho v_\rho^{(s)}) = 0, \\ v_z^{(s)}\frac{\partial v_z^{(s)}}{\partial z} + v_\rho^{(s)}\frac{\partial v_z^{(s)}}{\partial \rho} = \frac{R_s^{-1}}{\rho}\frac{\partial}{\partial \rho}\left(\rho\frac{\partial v_z^{(s)}}{\partial \rho}\right) \end{aligned}\right\} \quad (37a, b)$$

These equations are the analogues of (21 a, b) for the boundary layer on the sphere, although we have not yet formally introduced any thin-layer scales. The fluid emerges from the eruption region to form a jet whose initial diameter is $O(R_s^{-\frac{1}{4}})$ with $v_z^{(s)} = O(1)$. At distances $O(1)$ from the sphere, in the jet, we write $\rho = R_s^{-\frac{1}{4}}\tilde{\rho}, v_z^{(s)} = \tilde{u}$, $v_\rho^{(s)} = R_s^{-\frac{1}{4}}\tilde{v}$, so that, to first order, (37 a, b) become

$$\left.\begin{aligned} \frac{\partial}{\partial z}(\tilde{\rho}\tilde{u}) + \frac{\partial}{\partial \tilde{\rho}}(\tilde{\rho}\tilde{v}) = 0, \\ \tilde{u}\frac{\partial \tilde{u}}{\partial z} + \tilde{v}\frac{\partial \tilde{u}}{\partial \tilde{\rho}} = 0. \end{aligned}\right\} \quad (38a, b)$$

Equation (38 a) is satisfied if we introduce a stream function $\tilde{\psi}$ such that $\tilde{\rho}\tilde{u} = \partial\tilde{\psi}/\partial\tilde{\rho}$,

$\tilde{\rho}\tilde{v} = -\partial\tilde{\psi}/\partial z$, so that from (38*b*) $\tilde{u} = \tilde{u}(\tilde{\psi})$. It then follows, if $\tilde{\psi} = 0$ on $\tilde{\rho} = 0$ that $\tilde{\psi} = \tilde{\psi}(\tilde{\rho})$ since

$$\tilde{\rho}^2 = 2\int_0^{\tilde{\psi}} \frac{\mathrm{d}s}{\tilde{u}(s)},$$

with the consequence that $\tilde{v} \equiv 0$ to this order. Thus, on the scale of the sphere, the emergent jet behaves as an inviscid parallel flow. For this jet of thickness $O(R_s^{-\frac{1}{4}})$, it is only when we are at an axial distance $O(R_s^{\frac{1}{2}})$ from the sphere, with $v_z^{(s)} = O(1)$, $v_\rho^{(s)} = O(R_s^{-\frac{3}{4}})$ that the familiar thin viscous round jet emerges. The details of this are discussed by Schlichting (1955). The inviscid behaviour of the jet, described above, has features in common with the wake behind a steadily translating spherical gas bubble at high Reynolds number Re in a liquid. Thus Moore (1963) describes the inviscid behaviour of such a wake in a region of thickness $O(Re^{-\frac{1}{4}})$ extending over a distance downstream $O(Re^{\frac{1}{2}})$. The behaviour of our thin round jet is in marked contrast to the corresponding plane flow. For the case of a circular cylinder Riley (1987) establishes that the emergent jet, following a collision of the boundary layers, is one in which viscous effects are important even at distances $O(1)$ from the cylinder. Before we discuss the implications of this for the flow outside the boundary layer on the sphere, and the jet, we comment on the effect of the jet-flow for the force on the sphere.

In the complete absence of viscous effects the force which acts on a sphere in the presence of a fluctuating source is a force of attraction between source and sphere. Wang (1982) has shown that for $R_s \ll 1$ this attractive force is enhanced by an amount $O(\epsilon^2)$. However for the present case, with $R_s \gg 1$, the reverse is true since the jet which emerges along $\theta = 0$ is stronger than that along $\theta = \pi$, much stronger when the source is close to the sphere as figure 1 shows. There is then a net flux of momentum from the sphere towards the source which results in a net force of repulsion, $O(\epsilon^2/R_s^{\frac{1}{2}})$, between the source and the sphere.

We turn, finally, to the flow outside the boundary layers and jets. There the flow is inviscid and irrotational and, as may be inferred from (14), is governed by the equation

$$\mathrm{D}^2\psi_1^{(s)} = 0. \tag{39}$$

The appropriate solution of this equation is

$$\psi_1^{(s)} = \sum_{n=0}^{\infty} C_n r^{-n} Q_n(\mu). \tag{40}$$

The boundary condition from which the constants C_n are to be determined is provided by the viscous entrainment velocity into the boundary layers and jets. However, as we have argued above, entrainment into the jets is negligible by comparison with the entrainment into the boundary layers on the sphere. Consequently we have, for (40),

$$\frac{\partial\psi_1^{(s)}}{\partial\mu} = -v_\infty \quad \text{at } r = 1,$$

and hence

$$C_n = -\frac{2n+1}{2}\int_{-1}^{1} v_\infty(\mu)\, P_n(\mu)\,\mathrm{d}\mu.$$

Streamline patterns in this outer region, for various values of R, are shown in figure 6. We see how the distortion of the streamlines, as R decreases, reflects the distortion of the entrainment velocity shown in figure 4, and further demonstrates the increasing vigour of the fluid motion on the source-side of the sphere.

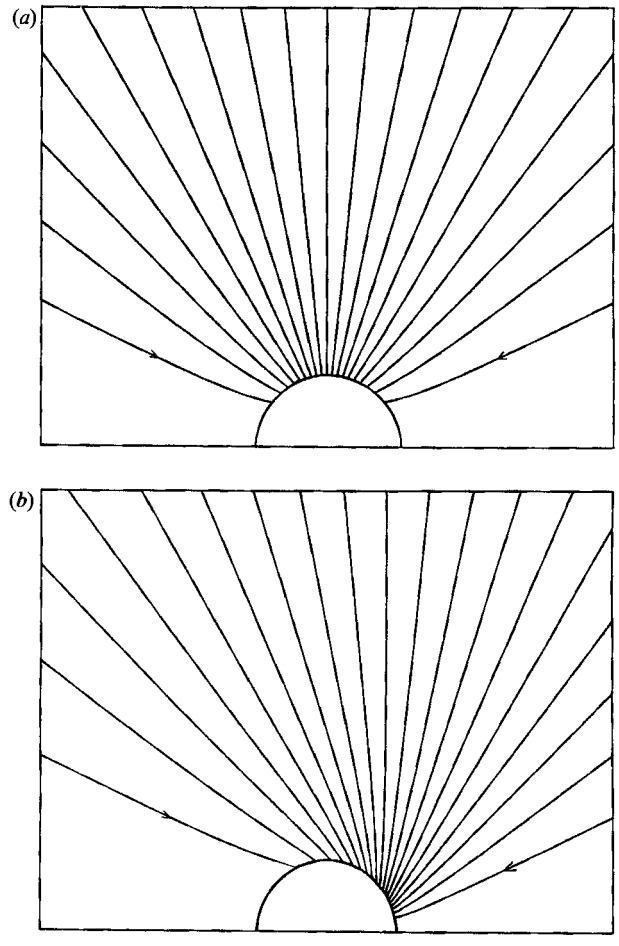

FIGURE 6. The outer, inviscid, mean streamlines for $R_s \gg 1$. In each case the streamlines are plotted at equal intervals $\delta\psi$ of $\psi_1^{(s)}$. (*a*) $R = \infty, \delta\psi = 0.126$; (*b*) $R = 1.5, \delta\psi = 0.361$.

Throughout the discussion in this section we have neglected the effect of any finite outer boundary to the domain. For two-dimensional flow Bertelsen's (1974) careful experiments show a small discrepancy between the measured velocity profiles close to the cylinder, and those predicted by theory for an unbounded domain. Duck & Smith (1979) and Haddon & Riley (1979) have demonstrated that this discrepancy may be explained, in part anyway, by the presence of an outer boundary.

4. An elementary experiment

An experimental verification of the flow analysed above, when a pulsating source is placed close to a solid sphere, is beyond our capabilities. However, there is one special case, namely the case in which the source is placed at infinity, when an elementary experiment can be performed. This simply corresponds to the case in which the sphere performs translational vibrations in a fluid which is otherwise at rest. Since the emergence of a thin round jet along the axis of vibration has not, apparently, been previously recorded we have thought it worthwhile to demonstrate this particular feature.

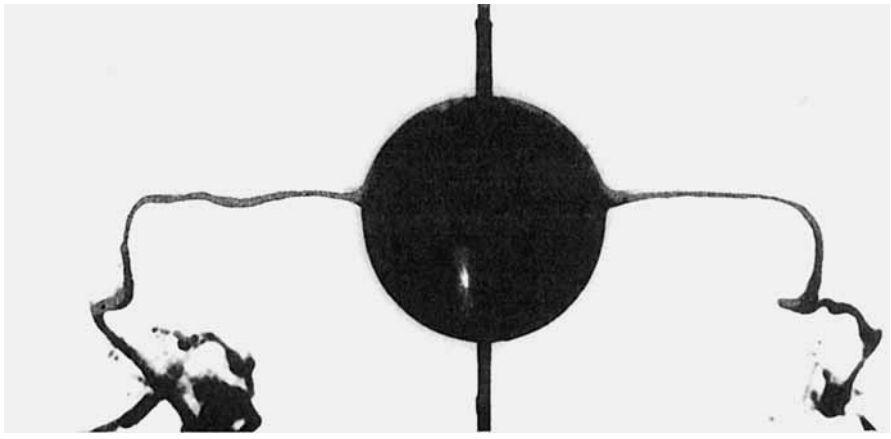

FIGURE 7. An example of the visualized jet flow.

The experiment was carried out in water in a glass-sided tank of length 75 cm, breadth 30 cm, and depth 37 cm. A polystyrene ball was mounted halfway along a flexible welding rod of diameter 0.2 cm and length 53 cm. The rod was fixed to the base of the tank and perpendicular to it. Although the upper end of the rod was free, a weight attached to it effectively anchored it. A horizontal shaft, which performed small-amplitude in-line vibrations, was attached to the rod one-quarter of its length from the top.

In the experiments, the sphere of diameter 4 cm, was vibrated at 17 Hz, and with a peak-to-peak amplitude of vibration of it in the range 0.2–0.3 cm, streaming Reynolds numbers $O(10^2)$ were realized. To visualize the flow a dye was introduced, via a hypodermic needle, to provide a thin coating over the upper hemisphere whilst at rest. The oscillatory motion was then begun. The dye drifted towards the stagnation points in a striking manner. From these stagnation points, where the dye accumulated, the axial jet was seen to form quite quickly and move out along the axis of vibration. However, to achieve a quasi-steady state with the jet stretched out along the axis of oscillation has proved less easy than in the plane case visualized by Davidson & Riley (1972). The principal difficulty was associated with unsteady start-up effects from which the dye tended to obscure the subsequent quasi-steady jet. To overcome this the dye was made slightly heavier than the host liquid so that the initial disturbance fell away. A typical visualization of the jet flow is shown in figure 7. Although no quantitative measurements were made, dye particles appeared to move with uniform speed in the jet, as would be the case in an effectively inviscid flow. However, more detailed measurements are required to confirm this.

N.A. acknowledges financial support by Universiti Teknologi Malaysia, and the Public Services Department of Malaysia, during the period in which this work was carried out.

REFERENCES

AMIN, N. 1989 Oscillation-induced mean flows and heat transfer. PhD thesis, University of East Anglia.

AWANG, M. A. O. 1984 Improved calculations for the steady flow over a heated sphere at high Grashof number. *J. Math. Phys. Sci.* **18**, 115–125.

BERTELSEN, A. F. 1974 An experimental investigation of high Reynolds number steady streaming generated by oscillating cylinders. *J. Fluid Mech.* **64**, 589–597.

BROWN, S. N. & SIMPSON, C. J. 1982 Collision phenomena in free-convective flow over a sphere. *J. Fluid Mech.* **124**, 123–137.

DAVIDSON, B. J. & RILEY, N. 1972 Jets induced by oscillatory motion. *J. Fluid Mech.* **53**, 287–303.

DUCK, P. W. & SMITH, F. T. 1979 Steady streaming induced between oscillating cylinders. *J. Fluid Mech.* **91**, 93–110.

HADDON, E. W. & RILEY, N. 1979 The steady streaming induced between oscillating circular cylinders. *Q. J. Mech. Appl. Maths* **32**, 265–282.

LIGHTHILL, M. J. 1978 Acoustic streaming. *J. Sound Vib.* **61**, 391–418.

MOORE, D. W. 1963 The boundary layer on a spherical gas bubble. *J. Fluid Mech.* **16**, 161–176.

NYBORG, W. L. 1953 Acoustic streaming equations: laws of rotational motion for fluid elements. *J. Acoust. Soc. Am.* **25**, 938–944.

POTTER, J. M. & RILEY, N. 1980 Free convection from a heated sphere at large Grashof number. *J. Fluid Mech.* **100**, 769–783.

RAYLEIGH, LORD 1884 On the circulation of air observed in Kundt's tubes, and on some allied acoustical problems. *Phil. Trans. R. Soc.* A **175**, 1–21.

RILEY, N. 1966 On a sphere oscillating in a viscous fluid. *Q. J. Mech. Appl. Maths* **19**, 461–472.

RILEY, N. 1967 Oscillatory viscous flows: review and extension. *J. Inst. Maths Applics* **3**, 419–434.

RILEY, N. 1987 Streaming from a cylinder due to an acoustic source. *J. Fluid Mech.* **180**, 319–326.

SCHLICHTING, H. 1955 *Boundary Layer Theory*. Pergamon.

STUART, J. T. 1963 *Laminar Boundary Layers*, chap. 7. Oxford University Press.

STUART, J. T. 1966 Double boundary layers in oscillatory viscous flow. *J. Fluid Mech.* **24**, 673–687.

WANG, C.-Y. 1972 Acoustic streaming of a cylinder near an unsteady source. *Recent Research on Unsteady Boundary Layers. IUTAM Symposium Quebec 1971*, pp. 1653–1678. Quebec, Laval University Press.

WANG, C.-Y. 1982 Acoustic streaming of a sphere near an unsteady source. *J. Acoust. Soc. Am.* **71**, 580–584.

WESTERVELT, P. J. 1953 The theory of steady rotational flow generated by a sound field. *J. Acoust. Soc. Am.* **25**, 60–67.